Sustainable Environmental Insight

Research Article
Volume 2(2), 2025, 124–140
https://doi.org/10.53623/sein.v2i2.767

Assessment of Heavy Metals, Microplastics Abundance, Pollution Level, and Contamination Risk in the Ganges Downstream

Md Ohidur Rahman[1], M. G. Mostafa[1]*, M. Sultan-Ul Islam[2], Shahed Zaman[3]

[1]Water Research Lab, Institute of Environmental Science, University of Rajshahi, Rajshahi 6205, Bangladesh
[2]Department of Geology and Mining, University of Rajshahi, Rajshahi 6205, Bangladesh
[3]Department of Chemistry, University of Rajshahi, Rajshahi 6205, Bangladesh

*Correspondence: mgmostafa@ru.ac.bd

SUBMITTED: 11 July 2025; REVISED: 3 September 2025; ACCEPTED: 8 September 2025

ABSTRACT: The degradation of aquatic ecosystems and their links to climate change had made microplastic (MP) contamination a significant environmental concern. The study evaluated the water quality and assessed the abundance, pollution level, and contamination risk of microplastics in the downstream of the Ganges. The analysis results revealed that biological oxygen demand, chemical oxygen demand, nitrate, and chromium levels slightly exceeded ECR-BD (2023) standards, reflecting mild pollution. Heavy metal analysis showed the following sequence of concentration: Fe > Cr > Cu > Ni > Pb > Zn > Mn > Cd, which increased gradually. Considering the water quality indices, the river water was moderately polluted. MP concentrations were higher in the pre-monsoon (17.7 particles/l) than in the post-monsoon (14.3 particles/l) season, with blue fibers <1 mm as the dominant forms. The identified MPs were polyethylene, polypropylene, polyethylene terephthalate, and polyvinyl chloride. The contamination factor (CF > 1) and the pollution load index (PLI > 1) indicated that the analyzed area was moderately contaminated with MPs. According to the study, the concentrations of Cr, Fe, and Cu increased with rising MP levels. Based on the co-occurrence of MPs and heavy metals, the Ganges River faced new ecological threats that needed to be addressed by tighter wastewater regulations, better plastic waste management, ongoing monitoring, and the implementation of transboundary policies to mitigate microplastic pollution.

KEYWORDS: Ganges downstream; surface water; microplastics; heavy metals; pollution

1. Introduction

Water Water pollution and its effects increased daily due to human activity. Several interrelated activities led to a rise in the production of hazardous pollutants, including heavy metals, organic pollutants, synthetic dyes, and microplastics, which contaminated the aquatic environment. These activities included mining, industrialization, agricultural runoff, and the expansion of residential areas [1]. Plastic emerged as a “miracle product,” and its accessibility increased because of special properties such as elasticity, durability, versatility, and cost-effectiveness, which made it widely available [2]. According to Plastics Europe [3], global plastic production

reached 413.8 million tons in 2023; only 3 million tons were bio-based and bio-attributed, while 36.2 million tons were produced from post-consumer recycled plastics. Plastic output was expected to nearly double or increase by approximately 70%, within the next two decades under a business-as-usual scenario [4]. As a result, aquatic environments were increasingly impacted by plastic waste.

Since 1972, several studies have advanced our knowledge of the characteristics, transport, and accumulation zones of oceanic plastic. Approximately 80% of oceanic plastic pollution originated from land-based sources, including wastewater treatment plant (WWTP) leaks, urban runoff, road drainage, atmospheric deposition, and the breakdown of larger plastic debris [5]. Freshwater systems served as a major downstream transport pathway for microplastics, linking inland and coastal communities to the ocean. Globally, rivers discharged between 0.4 and 265,000 million tons of plastic into coastal waters per year [6]. Microplastic (MP) particles emerged as a significant environmental pollutant of public and scientific concern, being small enough to be ingested by diverse marine organisms, from microscopic zooplankton to large vertebrate predators [7].

In recent years, global studies on riverine microplastic pollution grew rapidly. However, despite Asia being one of the most heavily impacted regions, rivers in Asian countries received comparatively less research attention. As a result, studies and field data on plastic pollution in major Asian rivers, such as the Ganges and Mekong, remained scarce [8]. In Bangladesh, the abundance and distribution of microplastics were occasionally reported in beach sediments, landfill soils, sea salt, rivers [9], and fish [10]. To the best of our knowledge, despite Bangladesh's freshwater and coastal ecosystems being heavily contaminated with plastic waste and highly susceptible to MP pollution, few studies were conducted on river water to evaluate MP levels and their implications for aquatic and human health.

The Ganges is referred to as the Padma and Meghna in Bangladesh, while in India it is called the Ganga. Research on microplastic pollution in the Ganges River remained scarce. A recent study tracked PET bottles through the Ganges River system into the Bay of Bengal using satellite and GPS cellular technology [11]. Additionally, discarded fishing gear represented a major source of plastic pollution in the Ganges River system [7]. However, no combined research addressed both microplastic and heavy metal pollution in the downstream Ganges. This study aimed to characterize water quality and to assess heavy metals, microplastic abundance, contamination levels, and associated risks in the downstream Ganges River across six locations (agricultural, fishing, rural, urban, and additional agricultural activity sites). The findings provided insight into the status of microplastic pollution in the downstream Ganges ecosystem and offered a basis for addressing the environmental challenges of the region.

2. Materials and Methods

2.1. Study area.

The study was conducted downstream of the River Ganga, from Godagari (24.45060°N, 88.34280°E) to Charghat (24.28330°N, 88.77500°E), Rajshahi, Bangladesh (SM Figure 1). The transboundary River Ganga flows from India and enters Bangladesh through the Nawabganj district in the western region. Originating from the Gangotri glacier in the Himalayas (Uttarakhand, India) at an elevation of nearly 7010 m, the river traverses about 2575 km before flowing southeast, branching into distributaries, and ultimately draining into the Bay

of Bengal [12]. Along its course, the river receives inputs from several large and small tributaries carrying substantial amounts of solid and liquid waste from industrial, commercial, residential, urban, and agricultural sources in both India and Bangladesh.

2.2. Sample collection, preparation, and analysis.

Surface water samples were collected from six sampling sites (RWS-1 to RWS-6) of the Ganges River in Bangladesh using the grab sampling method during the pre-monsoon (May–June) and post-monsoon (October–December) seasons of 2023 and 2024 to capture temporal variation in microplastic abundance. At each site, 100 L of river water was collected at a depth of ~0.5 m using a 10-l bucket. The water was filtered sequentially through 5 mm and 53 µm sieves. The solids retained on the 53 µm sieve were rinsed with distilled water into glass jars. All samples were collected in triplicate. To reduce cross-contamination, sieves were thoroughly rinsed with distilled water after each use. Samples were stored in iceboxes and immediately transported to the IES laboratory for analysis. Sampling locations are shown in SM Figure 1.

In situ parameters were measured on-site: temperature, pH, electrical conductivity (EC), and total dissolved solids (TDS) using a YSI Pro1030 multimeter (Xylem Inc., USA); dissolved oxygen (DO) with a Lutron DO-5509 meter (Lutron Electronics Co., Ltd., Taiwan); and turbidity with a Lutron TU-2016 meter (Lutron Electronics Co., Ltd., Taiwan). Additional samples were collected for analysis of major ions, heavy metals, and physicochemical characteristics. Total suspended solids (TSS), total hardness (TH), biochemical oxygen demand (BOD), chemical oxygen demand (COD), chloride (Cl^-), and bicarbonate (HCO_3^-) were determined using standard methods [13].

For cation and heavy metal analysis, water was collected in two 500 ml plastic bottles, sealed, and stored in iceboxes to prevent oxidation. Samples were filtered and acidified with concentrated HNO_3 (Fluka Analytical, Sigma-Aldrich, Germany). For digestion, 100 mL of water was treated with 2 ml concentrated HNO_3 and 3 ml concentrated HCl (MERCK, Germany). Major cations (Na^+, Mg^{2+}, Ca^{2+}) and heavy metals (Cr, Mn, Fe, Ni, Cu, Zn, Cd, Pb) were analyzed using an atomic absorption spectrophotometer (AAS-220FS, Shimadzu, Japan). Anions (PO_4^{3-}, NO_3^-, SO_4^{2-}) were analyzed with a UV-VIS spectrophotometer (VWR UV 6300PC, Avantor, USA) at the Rajshahi University Central Laboratory. Polymer types of isolated MPs were identified using Fourier Transform Infrared (FTIR) Spectroscopy (PerkinElmer 100 FTIR, PerkinElmer Inc., USA). Statistical analyses were performed using SPSS v20, while ArcGIS v10 was used for kriging interpolation. Basic statistical measures (mean, standard deviation) and water quality indices were calculated using Microsoft Excel.

2.3. Isolation, observation, and characterization of MPs.

The Microplastics were isolated following the U.S. National Oceanic and Atmospheric Administration (NOAA) protocol, involving four steps: (a) wet peroxide oxidation, (b) sequential sieving, (c) density separation, and (d) MP detection. Each sample was treated with 20 mL of 30% H_2O_2 (MERCK, Germany) and 20 mL of 0.05 M $FeSO_4$ (MERCK, Germany) for wet peroxide oxidation. Digestion was carried out on a hotplate in a fume hood at 75 °C. After cooling, 6 g of NaCl was added to 20 ml of solution (5 M NaCl) to increase the density. MPs floated and were separated using a density separator [14].

Filtered residues were collected using a vacuum pump with Whatman GF/C glass microfiber filters (1.2 µm pore size). The separated MPs were visually identified and

categorized by color, shape, and size using an Optika digital binocular microscope (B-190TB, 100×, Italy) equipped with a 3.2 MP tablet camera. MPs were classified by size into four categories: C1 (<1.0 mm), C2 (1.0–1.9 mm), C3 (2.0–2.9 mm), and C4 (≥3.0 mm). Based on morphology, MPs were categorized as film, fiber, fragment, or granule, and their colors identified as blue, red, green, violet, brown, or transparent.

The morphology, surface roughness, and elemental composition of MPs were further characterized using Scanning Electron Microscopy–Energy Dispersive X-ray Spectroscopy (SEM-EDS). Samples were coated with a DII-29030 SCTR Smart Coater (JEOL, Japan) and analyzed using a FE-SIGMA VP scanning electron microscope (Carl Zeiss Microscopy GmbH, Germany) coupled with two EDS detectors (Quantax XFlash 6|10, Bruker Nano GmbH, Germany). Polymer composition was confirmed by FTIR spectroscopy (PerkinElmer 100 FTIR, PerkinElmer Inc., USA).

2.4. Contamination factor and pollution load index.

Pollution load index (*PLI*) and contamination factors *(CFs*) are used to measure the level of contamination in natural ecosystems [15]. The *CF* values were classified into four groups: *CF* < 1 for low contamination, 1-3 for moderate contamination, 3-6 for considerable contamination, and > 6 for extremely high contamination. Conversely, when *PLI* >1, the sampling area is considered to be contaminated [15]. The demarcation of the valuation model was as follows:

$$CF = C_i / C_0 \quad (1)$$

$$PLI = (CF_1 \times CF_2 \times CF_3 \times .....CF_n)^{1/n} \quad (2)$$

Where C_i/C_0 is the proportion of the noted MP concentration vs. the contextual value. The lowest MP concentration of this investigation (0.34 particles/l in water) was utilized in place of the contextual value since the background value was unavailable [16, 17].

2.5. Indices approaches.

The water quality index (*WQI*), heavy metal evaluation index (*HEI*), and heavy metal pollution index (*HPI*) were utilized to assess the water quality in the study area. Metal concentrations were taken into consideration when calculating water quality indices.

2.5.1. WQI.

The study used the weighted arithmetic index approach to calculate *WQI* [18]. The *WQI* was computed using the following formula:

$$WQI = \frac{\sum W_i Q_i}{\sum W_i} \quad (3)$$

A value inversely equal to the suggested typical (*Si*) of the respective parameter was used to determine the relative weight (*Wi*) as follows:

$$Wi = 1/Si \quad (4)$$

The quality rating scale for each parameter, *Q*, was calculated by using the following expression:

$$Q_i = 100 \times \frac{V_n - V_i}{V_s - V_i} \quad (5)$$

Where V_n = the actual amount of the nth parameter and V_i= the ideal value of this parameter. *Vi*=0, except for pH (*Vi*=7.0) and DO (*Vi*=14.6 mg/L). *Vs* is the recommended standard of the corresponding parameter. According to the *WQI* value, water is classified into three categories: excellent (<50), good (50–100), bad (100–200), and 200 to 300 is really bad water [16].

2.5.2. HPI.

Two primary segments were involved in developing the *HPI* index, utilizing the weighted arithmetic mean process: choosing the pollution parameters that the index would be based on and creating a grading scale for each specified quality attribute that assigned weight to the selected parameters [19]. The rating scale (system) or unit weight (*Wi*) for metal concentration units of ppb was an arbitrary value (ranging from zero to one) that was computed as the inverse of the maximum allowable concentration (MAC). The maximum acceptable concentration (MAC) values of Cr, Mn, Fe, Ni, Cu, Zn, Cd, and Pb were 0.05, 0.40, 1.0, 0.05, 1.50, 5.0, 0.003, and 0.05 mg/L in that order [22]. We used the following equation to calculate *HPI*:

$$HPI = \frac{\sum_{i=1}^{n} W_i Q_i}{\sum_{i=1}^{n} W_i} \quad (6)$$

where *Qi* = the sub-index of the *i*th parameter, *Wi* = the unit weight of the *i*th parameter, and *n* = the number of parameters. *Qi* was calculated as below:

$$Qi = \sum_{i=1}^{n} \frac{|M_i - I_i|}{S_i - I_i} \times 100 \quad (7)$$

Where *Mi*, *Ii*, and *Si* are the monitored heavy metal, the ideal, and standard values of the *i*th parameter, respectively. The negative algebraic sign was omitted in the difference between *Mi* and *Ii*. The *Ii* values were taken from the MAC values of the metals, and the Si values were from the standard values set by the Bangladesh Environmental Conservation Rules (BECR), 2023. Water is categorized by Bhuiyan et al. [20] using a range of *HPI* values: *HPI* < 50 indicates minimal pollution, *HPI* = 50 -100 indicates moderate pollution, and *HPI* > 100 indicates elevated pollution.

2.5.3. HEI.

HEI gave an overall water quality assessment for heavy metals, and was computed as follows:

$$HEI = \sum_{i=1}^{n} \frac{H_c}{H_{MAC}} \quad (8)$$

Where H_c = the monitored value and H_{MAC} = the maximum admissible concentration (MAC) of the ith parameter. Water is categorized according to its *HEI* value: *HEI* < 10 indicates low pollution, *HEI* =10-20 indicates moderate pollution, and *HEI* > 20 indicates high pollution [21].

3. Results and Discussion

3.1. Characterization of river water.

The analysis results for physicochemical parameters and major ions are presented in Table 1. Most of the parameters complied with the Environmental Conservation Rules of Bangladesh (ECR-BD, 2023). Temperature, an important physiological regulator that strongly influences the behavior, growth, feeding, digestion, and productivity of aquatic organisms, remained within the standard limits and was favorable for aquatic life. pH, one of the most widely used indicators for evaluating water quality because of its role in both chemical and biological processes, ranged from 7.8 to 8.6 in this study. This range was generally acceptable; however, values at RWS-1 and RWS-2 slightly exceeded the upper limit (8.5), indicating that the river water was mildly alkaline. Such conditions remained favorable for fish and other aquatic organisms.

Table 1. Physicochemical parameters and major ions of river water.

Sample	RWS-1	RWS-2	RWS-3	RWS-4	RWS-5	RWS-6	*ECR- BD 2023
Temp.℃	22.5	24.6	24.5	22.1	22.5	23.8	20-30
pH	8.6	8.5	8.4	8.1	8.3	7.8	6.5-8.5
EC (µS/cm)	263	308	347	316	274	260	2250
TSS (mg/l)	28.1	31.4	37.5	22.8	20.1	18.9	50
TDS (mg/l)	201	244	262	245	222	215	1000
Turb. (NTU)	22.5	21.3	18.9	14.6	21.7	13.4	70
TH (mg/l)	135	150	150	160	155	135	500
DO (mg/l)	9.5	8.5	9.5	7	7.5	6.5	≥ 5
BOD (mg/l)	18	21	23	26	21	20	<12
COD (mg/l)	43	50	56	62	50	47	50
Na^+ (mg/l)	25.9	24.5	30.1	30.8	26	31.2	200
Ca^{2+} (mg/l)	38	40	42	48	40	36	75
Mg^{2+} (mg/l)	9.76	13.42	10.98	9.76	13.42	10.98	30-35
Cl^- (mg/l)	23.58	23.58	24.99	24.99	25.94	23.58	250
HCO_3^- (mg/l)	200	219	219	255	237	219	500
NO_3^- (mg/l)	7.11	9.39	8.69	5.14	4.19	3.56	07
PO_4^{3-} (mg/l)	1.59	1.87	1.99	1.33	1.10	1.63	05
SO_4^{2-} (mg/l)	32.36	33.55	35.11	34.33	33.11	32.36	200

*ECR- BD 2023 = Bangladesh Environmental Conservation Rule Report- 2023

The The turbidity (13.4–22.5 NTU), total suspended solids (8.9–37.5 mg/l), total hardness (135–160 mg/l), electrical conductivity (260–347 µS/cm), and total dissolved solids (201–262 mg/l) were within the standard ranges, indicating freshwater with carbonate–bicarbonate dominance, which supports fish growth. In aquatic ecosystems, calcium and magnesium are typically present as carbonates and bicarbonates, serving as essential nutrients for the development of fish scales and bones.

Dissolved oxygen (DO) strongly influences the survival, growth, behavior, and physiological efficiency of aquatic organisms and is typically depleted during microbial decomposition of organic matter. In this study, DO values (6.5–9.5 mg/l) were favorable for aquatic life. In contrast, biochemical oxygen demand (18–26 mg/l) exceeded the standard (<12 mg/l) at all sites, and chemical oxygen demand (56–62 mg/l) surpassed limits in some cases, reflecting organic and nutrient enrichment, likely from wastewater or agricultural runoff [22]. Elevated nitrate concentrations at RWS-2 and RWS-3 may have resulted from fertilizers, geological sources, decomposition of organic residues, domestic and municipal effluents, and agricultural runoff [22, 26].

Overall, the river water was mildly polluted. While most parameters remained within acceptable thresholds, elevated BOD, COD, and nitrate highlighted anthropogenic pressures that could accelerate eutrophication and impose ecological stress, underscoring the need for stronger pollution management.

3.2. Correlation analysis of the parameters.

A Correlation analysis was applied to examine relationships among physicochemical parameters (SM Table 1). A strong positive correlation was observed between TSS and NO_3^- (r = 0.934), indicating that particulate matter acted as a major nitrate carrier, likely linked to organic debris and runoff. Similarly, BOD showed strong correlations with COD (r = 0.996) and Ca^{2+} (r = 0.919), suggesting that organic loading was associated with oxidizable contaminants and calcium-rich inputs, most likely from agricultural or domestic sources. COD also correlated strongly with EC (r = 0.767) and TDS (r = 0.797), highlighting the contribution of conductive and dissolved materials to organic pollution.

Dissolved oxygen correlated negatively with HCO_3^- (r = –0.633), but positively with pH (r = 0.884), TSS (r = 0.859), and NO_3^- (r = 0.817). This indicated that oxygen availability increased alongside nutrient enrichment and algal activity, while elevated bicarbonate concentrations reflected buffering capacity that could suppress oxygen levels. Turbidity correlated positively with both DO (r = 0.718) and pH (r = 0.908), suggesting that photosynthetic activity influenced both water clarity and oxygen dynamics.

Among the major ions, Ca^{2+} exhibited strong positive correlations with TH (r = 0.840), BOD (r = 0.919), and COD (r = 0.924), confirming its role in hardness and its link with organic inputs. HCO_3^- also showed strong correlations with TH (r = 0.842) and BOD (r = 0.850), consistent with carbonate–bicarbonate dominance and organic pollution. Additionally, PO_4^{3-} correlated strongly with TSS (r = 0.802) and NO_3^- (r = 0.762), indicating that suspended matter and agricultural runoff were key contributors to nutrient enrichment.

3.3. Heavy metals analysis.

The concentrations of heavy metals in river water are summarized in Table 2. Iron (Fe) showed the highest concentration (0.16–0.20 mg/l), while cadmium (Cd) exhibited the lowest (0.017–0.020 mg/l). Overall, the distribution of heavy metals followed the decreasing order: Fe > Cr > Cu > Ni > Pb > Zn > Mn > Cd.

Table 2. Statistical analysis of heavy metals in river water.

Sample (mg/l)	RWS-1	RWS-2	RWS-3	RWS-4	RWS-5	RWS-6	*ECR- BD 2023
Cr	0.1007	0.1032	0.1102	0.1014	0.1031	0.1061	0.1
Mn	0.0112	0.0201	0.0209	0.0256	0.0188	0.0216	02
Fe	0.1692	0.1707	0.1908	0.1993	0.1931	0.1599	03
Ni	0.0774	0.0742	0.0833	0.0647	0. 0742	0.0615	0.1
Cu	0.0803	0.0712	0.0955	0.0966	0.0793	0.0736	03
Zn	0.0171	0.0211	0.0201	0.0273	0.0255	0.0314	05
Cd	0.01919	0.01838	0.01999	0.01817	0.01733	0.01711	.03
Pb	0.0326	0.0253	0.0354	0.0309	0.0236	0.0337	0.1

*ECR- BD = Bangladesh Environmental Conservation Rule Report- 2023.

Nonetheless, the concentrations of most elements, including Mn, Fe, Ni, Cu, Zn, Cd, and Pb, were within the ECR-BD (2023) recommended standards. However, the concentrations of Cr exceeded the permissible limit of 0.1 mg/l. The results indicated that heavy metal concentrations increased gradually. The elevated levels were likely attributed to untreated sewage and domestic waste discharges, along with industrial and agricultural runoff.

3.4. Indices analysis.

One One of the most effective approaches to describe overall water quality is the WQI, which condenses large datasets into a single value between 0 and 100 [23]. Water quality and pollution-level classifications for the WQI, HEI, and HPI are presented in SM Table 2. The calculated WQI values ranged from 57.51 to 66.23, indicating that the river water quality was generally good (Figure 2). Heavy metal pollution levels were assessed using HPI and HEI indices for eight metals (Cr, Mn, Fe, Ni, Cu, Zn, Cd, and Pb). The HPI values ranged from 50.52 to 59.67, while the HEI values ranged from 2.63 to 3.06 (Figure 1). Based on the HPI classification, the river water was moderately polluted by heavy metals, consistent with the findings of Bhuiyan et al. (2010) [20].

The HEI provided additional insight into the degree of contamination, linking heavy metal concentrations to toxicity levels and thereby offering information about potential risks to aquatic biota. According to HEI values, the river water had a low level of heavy metal pollution [20]. According to a report, agriculture and other human-caused activities are the main producers of plastic and other pollutants in river water [24]. Urbanization and population density have an impact on the amount of microplastic contamination.

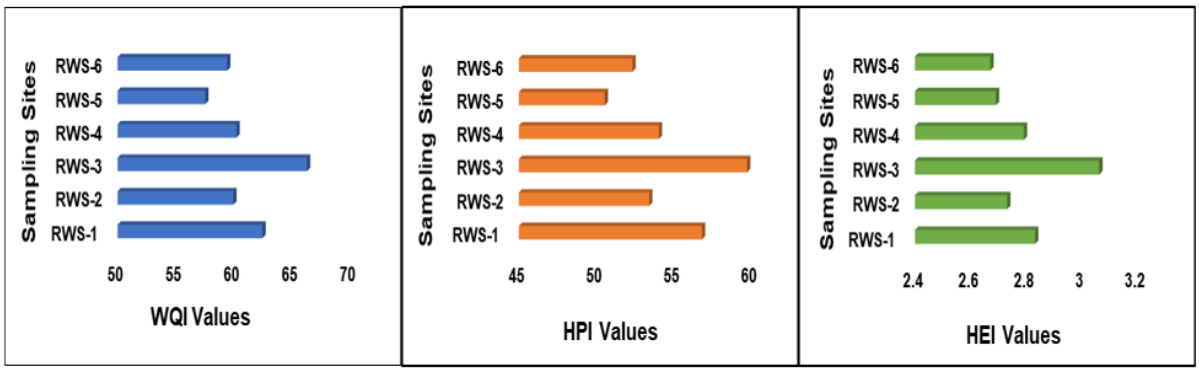

Figure 1. Water quality indices: a) WQI; b) HPI; and c) HMEI.

3.5.Abundance and distribution of MPs.

Microplastics (MPs) isolated from the water samples are shown in Figure 2. The microplastic (MP) content in the water samples ranged from 13.4 to 15.2 particles/l, with an average of 14.3 ± 0.7 particles/l during the post-monsoon season and from 15.6 to 21.5 particles/l, with an average of 17.7 ± 2.1 particles/l during the pre-monsoon season in 2023. In 2024, MP content ranged from 13.8 to 16.0 particles/l (average 14.8 ± 0.8 particles/l) in the post-monsoon season and from 16.7 to 22.1 particles/l (average 18.6 ± 1.6 particles/l) in the pre-monsoon season. Overall, a greater abundance of microplastics was observed in the pre-monsoon compared to the post-monsoon season.

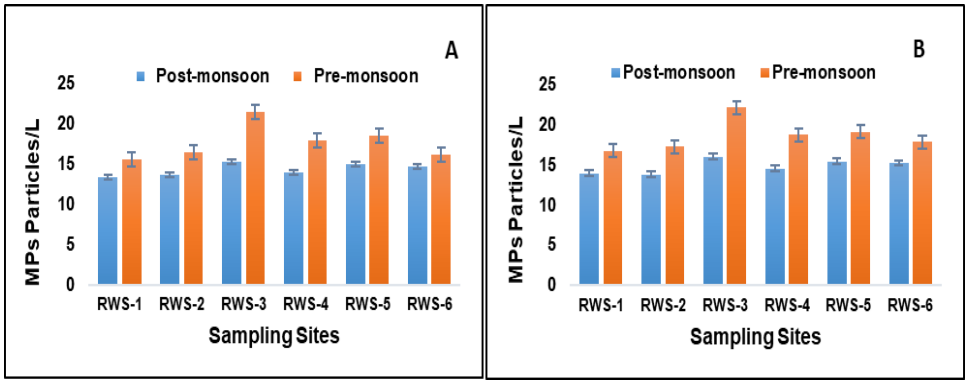

Figure 2. Average microplastics abundance in river water in 2023 (A) and 2024 (B).

The highest microplastic concentration was determined at RWS-3, and the lowest microplastic concentration was at RWS-1. Because of the dense residential and commercial areas, as well as the municipal sewage, the concentration of microplastics in the RWS-3 and RWS-5 was significantly higher than in the other locations. Additionally, areas with a high population density also had high levels of microplastics. Since the RWS-1 location is the most upstream station of the study, there were fewer MPs due to fishing and farming. Fishing and farming activities also resulted in lower MPs in the RWS-2 and RWS-6 locations. This is not surprising that plastic and other pollutants are primarily produced by agriculture and other human-caused activities [24]. Numerous biophysical and socioeconomic issues, such as pollution, flooding, erosion, salinization, and waterlogging, are affecting the river more frequently as a result of anthropogenic changes and climate change.

The abundance of microplastics (MPs) in our study area was lower than that reported in Indonesia's Ciwalengka River [14], China's Wei River [25], and the Meghna Estuary, Bangladesh [26]. Fewer MPs were documented by [27–28], whereas higher abundances were reported by [29] (SM Table 3). Variations in MP abundance across studies are strongly influenced by methodological factors such as sampling depth, net mesh size, and seasonal conditions. Sampling depth is critical, as buoyant polymers (PE, PP) concentrate near the surface, while denser types (PET, PVC) sink; thus, surface-only sampling may overestimate lighter MPs. Net mesh size also introduces bias, since coarser meshes (>300 μm) fail to capture smaller MPs, while finer meshes (<100 μm) detect more particles, yielding higher reported abundances [30]. Seasonal variation further affects MP levels: during the monsoon, high discharge and runoff increase inputs, while in the dry season, hydrodynamic conditions may promote surface accumulation. Biofouling can also alter MP buoyancy, depending on seasonal biological activity [30, 31]. Overall, MP concentrations in rivers vary widely worldwide due to differences in source loads, surrounding environments, hydraulic features, and waste generation patterns [16]. Based on these comparisons, MP pollution in the studied river can be classified as medium relative to other global rivers.

3.6. Correlation analysis between microplastics and heavy metals.

The correlation coefficients between microplastics (MPs) and heavy metals are displayed in a Pearson correlation matrix (Table 3). MPs are significant vectors for the transmission of pollutants due to their sorption capacity, motility, and persistence, which have consequences for ecotoxicology and contamination of the food chain. Their high surface-area-to-volume ratio, surface charges, and persistence (especially after aging) enable them to adsorb and carry

metals in aquatic environments [32]. Strong positive correlations (>0.5) were found between MPs and Cr, Fe, and Cu, suggesting possible shared sources. The relation indicated that Cr, Fe, and Cu were accumulated and transported by MPs from their sources. Microplastics (MPs) exhibit a strong affinity for Cr, Fe, and Cu through multiple mechanisms. Environmental aging (UV, oxidation, and mechanical abrasion) introduces oxygen- and nitrogen-containing groups (–COOH, –OH, –C=O, and amides) and roughens surfaces, thereby enhancing the metal adsorption capacity. Electrostatic attraction and inner-sphere complexation dominate, with deprotonated functional groups binding Cu^{2+}, Fe^{3+}, and Cr^{3+}. Cu^{2+} readily forms stable complexes with $–COO^{-}$/–OH groups, while the pH and dissolved organic matter of the solution regulate sorption. Cr sorption depends on speciation: Cr (VI) interacts through protonated sites or reduction to Cr (III), whereas Cr (III) complexes with surface ligands. Fe^{3+} hydrolysis produces Fe $(OH)_x$, which complexes with MPs or forms coatings, thereby further promoting sorption [33]. These findings highlighted that MPs have the potential to accumulate and transport metals, aiding in pollution source tracking and environmental risk.

Table 3. Pearson correlation matrix between microplastics (MPs) and heavy metals.

	MPs	Cr	Mn	Fe	Ni	Cu	Zn	Cd	Pb
MPs	1								
Cr	**0.714**	1							
Mn	0.381	0.294	1						
Fe	**0.696**	0.020	0.436	1					
Ni	**0.516**	0.316	-0.501	0.218	1				
Cu	**0.694**	0.232	0.383	0.784	0.211	1			
Zn	-0.107	0.072	0.679	-0.013	-0.869	-0.093	1		
Cd	0.461	0.319	-0.294	0.188	0.792	0.519	-0.816	1	
Pb	0.199	0.474	0.005	-0.179	0.023	0.455	-0.034	0.486	1

Bold numbers indicate a strong positive relationship.

3.7.Morphological characteristics of MPs.

3.7.1. Microscopic analysis.

The morphological properties of MP particles, including their color, size, and shape, were examined. Figure 3 shows distinctive microscopic images of the isolated MPs. The morphology of the isolated microplastics (color, Shape, and Size) of water samples in six different locations is shown in Figure 4.

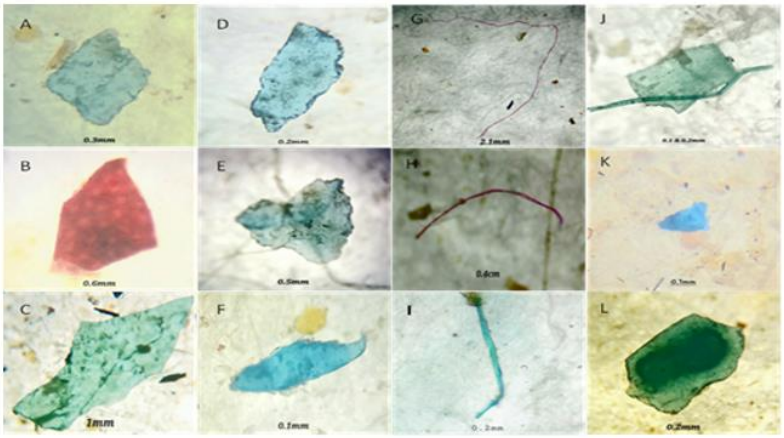

Figure 3. Typical image of isolated MPs (Magnification- 40x): Fiber (a, e); Film (d, f); Fragment (c, g); and Granule (d, h).

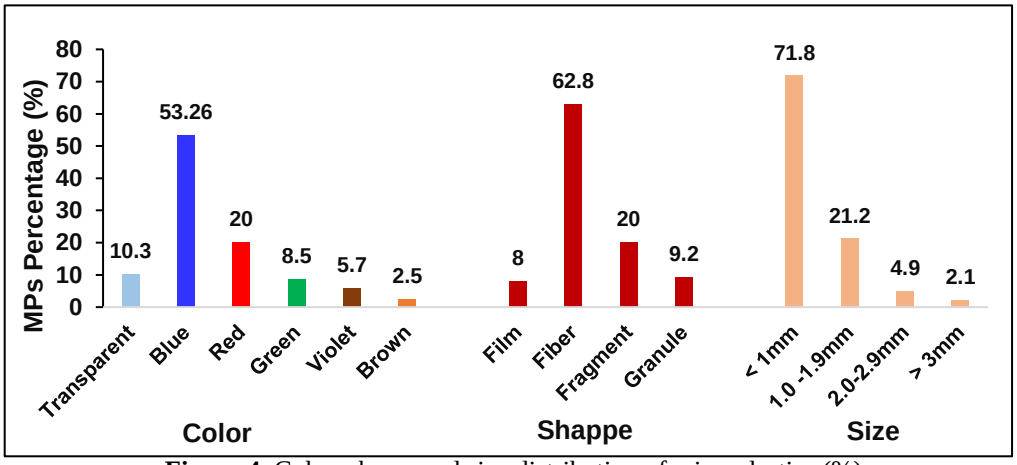

Figure 4. Color, shape, and size distribution of microplastics (%).

More than 85% of the MPs in the river water were colored, with blue being the most dominant (53%). The colors of MPs followed the descending order: blue > red > transparent > green > violet > brown. This wide variety of colors reflects the diversity of their sources. Notably, prolonged exposure to sunlight can cause colors such as red and blue from films and fibers to fade or lose intensity in aquatic environments. In terms of morphology, MPs were primarily composed of fibers (62.8%), with a mean concentration of 43 items/l across all sampling locations, followed by fragments (20%), granules (9.2%), and films (8%) (Figure 4). The highest recorded abundances of fibers (9.5 items/l), fragments (2.9 items/l), granules (1.3 items/l), and films (1.5 items/l) were observed at the RWS-3 location. De Falco et al. [34] suggested that fibers and fragments in aquatic systems often originate from the disintegration of fishing gear and the release of laundry wastewater. Regarding particle size, 71.8% of MPs were <1.0 mm, 21.2% were within 1.0–1.9 mm, and 7% were ≥2.0 mm. According to Wang et al. [24], this pattern likely reflects the breakdown of larger plastic items into smaller MPs through chemical, physical, and microbiological processes. These findings are consistent with results reported for the Karnaphuli River, Bangladesh [28].

3.7.2. SEM-EDX analysis.

The SEM-EDX investigations provided insights into the morphology, surface roughness, elemental composition, and types of minerals and metals accumulated on the surfaces of microplastic particles [35]. SEM images revealed irregular and rough areas on otherwise smooth surfaces of microplastics, indicating degradation processes (SM Figure 2). EDX results identified C, O, and Cl as the dominant elements, while Na, Al, Si, and K appeared as impurities. The detection of Na was attributed to the addition of NaCl during the density separation process, whereas Al and Si likely originated from sand in the river water. Although SEM-EDX is a powerful technique for identifying inorganic impurities associated with environmental matrices, the preparation process can introduce artifacts, such as salt residues, mounting substrates, and sputter-coating materials. To minimize misinterpretation, procedural blanks were analyzed under the same conditions. Nevertheless, soluble residues and trace contaminants cannot be completely ruled out, so the results should be considered indicative

rather than fully quantitative. These SEM-EDX analyses provided initial qualitative insights into the morphological characteristics of MPs.

3.7.3. FTIR analysis.

The FTIR spectra (Figure 5) were utilized to determine the polymer types of the microplastic samples through comparison of the distinctive absorption bands with established FTIR reference libraries. A spectral match criterion of at least 70% was deemed suitable for initial identification, while values exceeding 80% provided robust confirmation [36]. The presence of C–H stretching vibrations at 2915 and 2848 cm^{-1} and bending peaks close to 1471 and 719 cm^{-1} is acceptable for the identification of polyethylene (PE). Similar CH_2 stretching bands were seen in polypropylene (PP), but it was differentiated by extra CH_3 deformation peaks at 1455 and 1375 cm^{-1}. Strong carbonyl (C=O) stretching at 1717 cm^{-1}, aromatic C=C stretching at 1615–1500 cm^{-1}, and C–O vibrations in the 1240–1090 cm^{-1} range were the characteristics of polyethylene terephthalate (PET). Unique C–Cl stretching bands at 600–700 cm^{-1}, backed by CH_2 deformations at 1430 cm^{-1}, were used to identify polyvinyl chloride (PVC). Some overlaps were observed between PE and PP, particularly in the 2800–2900 cm^{-1} region due to common CH_2 vibrations. The presence of CH_3-related bands in PP, which are absent in PE, was one of several diagnostic peaks taken into consideration in order to resolve these discrepancies [37]. Therefore, the FTIR analyses indicated the presence of polyethylene (PE), polypropylene (PP), polyethylene terephthalate (PET), and polyvinyl chloride (PVC).

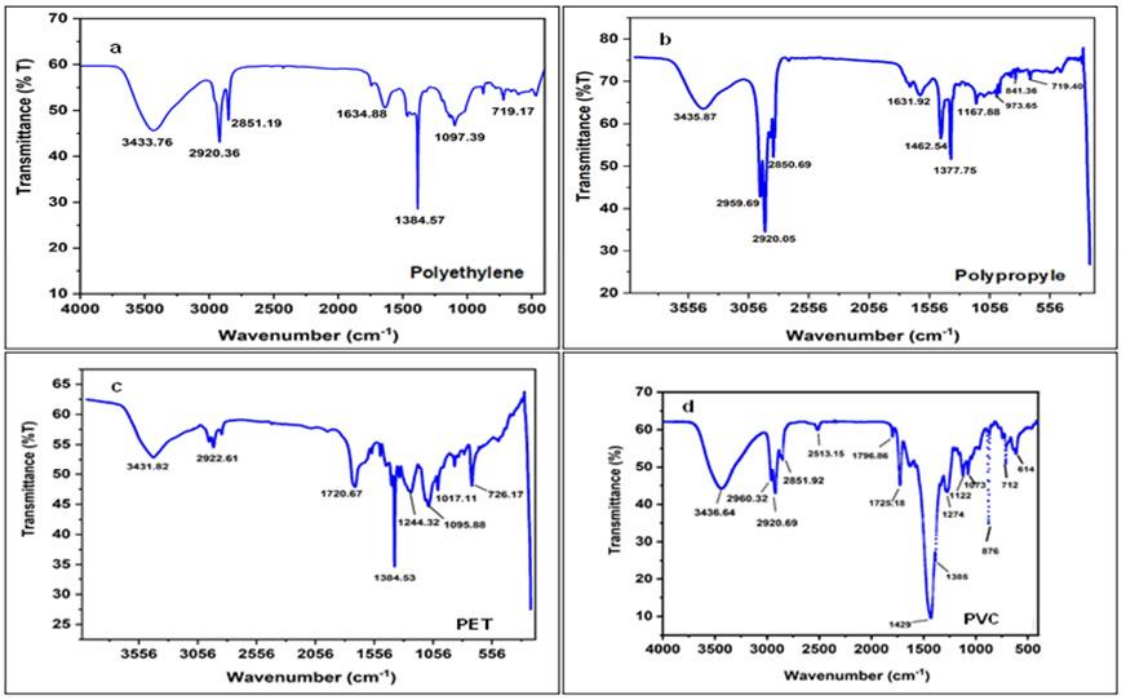

Figure 5. FTIR spectra of MPs isolated from river water samples: (a) polyethylene, (b) polypropylene, (c) polyethylene terephthalate (PET), and (d) polyvinyl chloride (PVC).

3.8.Analysis of contamination level in river water.

The contamination factor (CF) of the studied river samples is presented in SM Figure 3. The CF values (not shown in the table) ranged from 1.0 to 1.53, with an average of 1.27 ± 0.22, while the pollution load index (PLI) score was 1.40 ± 0.10. These CF and PLI values indicate moderate microplastic contamination—higher than pristine conditions (CF < 1; PLI ≤ 1) but

lower than levels observed in heavily impacted systems. In Bangladesh, CF values up to ~12 and PLI values around 3.5 have been reported in industrial zones [38], whereas Mohamaya Lake [39] exhibited moderate–high contamination. Seasonal variation also influenced MP loads, with higher CF and PLI values during dry seasons compared to wet periods, likely due to dilution effects. In tropical estuarine systems such as the Karnaphuli River Estuary, Bangladesh (PLI > 1) [16], MPs frequently fall into moderate-to-high risk categories. In comparison, the present results suggest localized but not severe anthropogenic inputs, primarily from municipal, agricultural, and small-scale urban sources. Overall, these values indicate an intermediate stage of MP pollution, highlighting the need for early management interventions and continuous monitoring.

3.9. Correlation analysis of MPs.

The correlation coefficients between film, fiber, fragment, and granule are presented in Table 4, where higher values indicate stronger positive correlations. A strong positive correlation (>0.5) was observed between film and fiber (0.61) and between film and granule (0.64). Similarly, fiber and granule exhibited a strong positive linear relationship (0.60). In contrast, film and fragment showed the weakest correlation (0.31). Such significant positive correlations help identify the origin of MPs, suggesting that different types of MPs often share common sources. Principal component analysis (PCA) further supported these relationships. The correlation matrix yielded two principal components (PCs) with eigenvalues greater than 1, together explaining 84.32% of the total variance (Table 4). The first principal component (PC1) accounted for the highest variability (56.1%) and showed strong positive correlations (>0.75) with film, fiber, and granule. These forms of MPs are commonly linked to domestic and municipal sources such as packaging materials, food wrappers, single-use plastics, synthetic textiles, and household products, as well as agricultural inputs like mulching films and fertilizer coatings. Their grouping within PC1 suggests mixed origins from wastewater discharge, urban runoff, and agricultural activities [19]. The second principal component (PC2), which accounted for 28.22% of the variance, showed a strong positive correlation with fragments, indicating a distinct source pathway. Fragments are typically derived from the secondary breakdown of larger plastic items (e.g., bottles, containers, and construction materials) through photodegradation and physical abrasion [40].

Table 4. Component matrix of the active variables.

Type	Film	Fiber	Fragment	Granule	PC1	PC2
Film	1				.885	.291
Fiber	**.612**	1			.843	-.242
Fragment	.306	-.106	1		.100	.977
Granule	**.644**	**.601**	-.066	1	.860	-.175
Eigenvalue					2.24	1.13
% Variance					56.10	28.22
Cumulative					56.10	84.32

(Bold numbers indicate a strong positive relationship).

4. Conclusion

This study provides an integrated assessment of physicochemical parameters, heavy metals, and microplastics (MPs) in river water, revealing multiple levels of pollution. While most parameters complied with ECR-BD (2023) standards, elevated BOD, COD, and NO_3^- in some samples indicated organic enrichment from anthropogenic and natural sources. Heavy metal

concentrations followed the order Fe > Cr > Cu > Ni > Pb > Zn > Mn > Cd, with Cr exceeding permissible limits. The WQI > 50, HPI > 50, and HEI < 10 collectively categorized the river as moderately polluted. MPs were detected year-round, with higher concentrations during the pre-monsoon season (17.7 particles/l) compared to the post-monsoon season (14.3 particles/l), particularly in areas of intense human activity. Most MPs were fibers, predominantly blue in color and <1 mm in size, indicating textiles and plastic debris as major sources. SEM-EDS and FTIR confirmed the presence of common polymers, including polyethylene (PE), polypropylene (PP), polyethylene terephthalate (PET), and polyvinyl chloride (PVC). Pearson's correlation analysis revealed strong associations between MPs and heavy metals, highlighting their role as vectors for contaminant transport. The contamination factor (CF > 3) and pollution load index (PLI > 1) indicated moderate MP contamination. Overall, the combined evaluation of water quality, heavy metals, and MPs points to a synergistic pollution scenario in which MPs not only act as emerging contaminants but also facilitate the accumulation of heavy metals, particularly Fe, Cr, and Cu. These findings underscore the dual ecological risks posed by MPs and heavy metals and highlight the urgent need for integrated management strategies to mitigate their combined impacts on river ecosystems.

Acknowledgment

One of the authors would like to thank the Institute of Environmental Science, University of Rajshahi, Rajshahi, Bangladesh, for providing him with a PhD fellowship. He also thanks the Ministry of Education for granting him deputation (study leave) to conduct his PhD research.

Declaration of competing interest

The authors declare that they have no known competing financial interests or personal relationships that could have appeared to influence the work reported in this paper.

Author contributions

Md Ohidur Rahman: Conceptualization, methodology, investigation, sample collection, sample analysis, data curation, data analysis, software computation, and writing the original draft. M.G. Mostafa: Conceptualization, methodology, investigation, project administration, validation, software, supervision, writing review & editing, and finally submission. M. Sultan-Ul-Islam: Conceptualization, Supervision, Writing review, and Editing. Shahed Zaman: Conceptualization, Supervision, Writing review.

Appendix A. Supplementary data

Supplementary data to this article can be found online at https://doi.org/10.53623/sein.v2i2.767.

References

[1] Tang, Y.; Liu, Y.; Chen, Y.; Zhang, W.; Zhao, J.; He, S.; Yang, Z. (2021). A review: Research progress on microplastic pollutants in aquatic environments. *Science of the Total Environment, 766*, 142572. https://doi.org/10.1016/j.scitotenv.2020.142572.

[2] Akter, M.S.; Chakraborty, T.K.; Ghosh, G.C.; Nice, M.S.; Zaman, S.; Khan, A.S. (2024). Microplastics and heavy metals in freshwater fish species in the southwestern region of

Bangladesh: An emerging concern for public health. *Emerging Contaminants*, *10*(3), 100325. https://doi.org/10.1016/j.emcon.2024.100325.

[3] Plastics Europe (2024). Circular Economy for Plastics – A European Analysis. https://plasticseurope.org/knowledge-hub/plastics-the-fast-facts-2024/.

[4] OECD (2024). Policy Scenarios for Eliminating Plastic Pollution by 2040. OECD Publishing, Paris. https://doi.org/10.1787/76400890-en.

[5] De Falco, F.; Cocca, M.; Avella, M.; Thompson, R.C. (2020). Microfiber release to water, via laundering, and to air, via everyday use: a comparison between polyester clothing with differing textile parameters. *Environmental Science & Technology*, *54*(6), 3288–3296. https://doi.org/10.1021/acs.est.9b06892.

[6] Mai, L.; et al. (2020). Global Riverine Plastic Outflows. *Environmental Science & Technology*, *54*(16), 10049–10056. https://doi.org/10.1021/acs.est.0c02273.

[7] Nelms, S.E.; et al. (2020). Riverine plastic pollution from fisheries: Insights from the Ganges River system. *Science of the Total Environment*, *743*, 143305. https://doi.org/10.1016/j.scitotenv.2020.143305.

[8] Chowdhury, G.W.; Koldewey, H.J.; Duncan, E.; Napper, I.E.; Niloy, M.N.H.; Nelms, S.E.; Sarker, S.; Bhola, S.; Nishat, B. (2021). Plastic pollution in aquatic systems in Bangladesh: A review of current knowledge. *Science of the Total Environment*, *761*, 143285. https://doi.org/10.1016/j.scitotenv.2020.143285.

[9] Islam, T.; Li, Y.; Rob, M.M.; Cheng, H. (2022). Microplastic pollution in Bangladesh: Research and management needs. *Environmental Pollution*, *308*, 119697. https://doi.org/10.1016/j.envpol.2022.119697.

[10] Hossain, M.B.; Pingki, F.H.; Azad, M.A.S.; Nur, A.A.U.; Banik, P.; Sarker, P.K.; Yu, J. (2024). Accumulation, tissue distribution, health hazard of microplastics in a commercially important cat fish, Silonia silondia from a tropical large-scale estuary. *Frontiers in Sustainable Food Systems*, *8*, 1372059. https://doi.org/10.3389/fsufs.2024.1372059.

[11] Duncan, E.M.; et al. (2020). Message in a bottle: Open-source technology to track the movement of plastic pollution. *PLOS ONE*, *15*(12), e0242459. https://doi.org/10.1371/journal.pone.0242459.

[12] Singh, R.; Singh, G.S. (2019). Integrated management of the Ganga River: An ecohydrological approach. *Ecohydrology & Hydrobiology*. https://doi.org/10.1016/j.ecohyd.2019.10.007.

[13] APHA (1998). Standard Methods for the Examination of Water and Wastewater, 20th Ed.; American Public Health Association, American Water Works Association and Water Environmental Federation: Washington DC, USA.

[14] Alam, F.C.; Sembiring, E.; Muntalif, B.S.; Suendo, V. (2019). Microplastic distribution in surface water and sediment river around slum and industrial area (case study: Ciwalengke River, Majalaya district, Indonesia). *Chemosphere*, *224*, 637–645. https://doi.org/10.1016/j.chemosphere.2019.02.188.

[15] Tomlinson, D.L.; Wilson, J.G.; Harris, C.R.; Jeffrey, D.W. (1980). Problems in the assessment of heavy-metal levels in estuaries and the formation of a pollution index. *Helgoländer Meeresuntersuchungen*, *33*, 566–575. https://doi.org/10.1007/bf02414780.

[16] Rakib, M.R.J.; Hossain, M.B.; Kumar, R.; Ullah, M.A.; Al Nahian, S.; Rima, N.N.; Sayed, M.M. (2022). Spatial distribution and risk assessments due to the microplastics pollution in sediments of Karnaphuli River Estuary, Bangladesh. *Scientific Reports*, *12*(1), 8581. https://doi.org/10.1038/s41598-022-12296-0.

[17] Li, R.; Yu, L.; Chai, M.; Wu, H.; Zhu, X. (2020). The distribution, characteristics and ecological risks of microplastics in the mangroves of Southern China. *Science of the Total Environment*, *708*, 135025. https://doi.org/10.1016/j.scitotenv.2019.135025.

[18] Tandel, B.N.; Macwan, J.E.M.; Soni, C.K. (2011). Assessment of water quality index of small lake in south Gujarath region, India. Proceedings of ISEM-2011, Thailand.

[19] Islam, M.Z.; Mostafa, M.G. (2024). Iron, manganese, and lead contamination in groundwater of Bangladesh: A review. *Water Practice & Technology*, *19*(3), 745–760. https://doi.org/10.2166/wpt.2024.030.

[20] Bhuiyan, M.A.; Islam, M.A.; Dampare, S.B.; Parvez, L.; Suzuki, S. (2010). Evaluation of hazardous metal pollution in irrigation and drinking water systems in the vicinity of a coal mine area of northwestern Bangladesh. *Journal of Hazardous Materials*, *179*(1–3), 1065–1077. https://doi.org/10.1016/j.jhazmat.2010.03.114.

[21] Tokatli, C.; Mutlu, E.; Arslan, N. (2021). Assessment of the potentially toxic element contamination in water of Şehriban Stream (Black Sea Region, Turkey) by using statistical and ecological indicators. *Water Environment Research*, *93*(10), 2060–2071. https://doi.org/10.1002/wer.1576.

[22] Haque, M.A.; Jewel, M.A.S.; Sultana, M.P. (2019). Assessment of physicochemical and bacteriological parameters in surface water of Padma River, Bangladesh. *Applied Water Science*, *9*, 1–8. https://doi.org/10.1007/s13201-018-0885-5.

[23] Tyagi, S.; Sharma, B.; Singh, P.; Dobhal, R. (2013). Water quality assessment in terms of water quality index. *American Journal of Water Resources*, *1*(3), 34–38. https://doi.org/10.12691/ajwr-1-3-3.

[24] Wang, F.; Wong, C.S.; Chen, D.; Lu, X.; Wang, F.; Zeng, E.Y. (2018). Interaction of toxic chemicals with microplastics: A critical review. *Water Research*, *139*, 208–219. https://doi.org/10.1016/j.watres.2018.04.003.

[25] Ding, L.; Fan Mao, R.; Guo, X.; Yang, X.; Zhang, Q.; Yang, C. (2019). Microplastics in surface waters and sediments of the Wei River, in the northwest of China. *Science of the Total Environment*, *667*, 427–434. https://doi.org/10.1016/j.scitotenv.2019.02.332.

[26] Alam, M.J.; Shammi, M.; Tareq, S.M. (2023). Distribution of microplastics in shoreline water and sediment of the Ganges River Basin to Meghna Estuary in Bangladesh. *Ecotoxicology and Environmental Safety*, *266*, 115537. https://doi.org/10.1016/j.ecoenv.2023.115537.

[27] Islam, M.S.; Islam, Z.; Hasan, M.R. (2022). Pervasiveness and characteristics of microplastics in surface water and sediment of the Buriganga River, Bangladesh. *Chemosphere*, *307*, 135945. https://doi.org/10.1016/j.chemosphere.2022.135945.

[28] Hossain, M.J.; AftabUddin, S.; Akhter, F.; Nusrat, N.; Rahaman, A.; Sikder, M.N.A.; Zhang, J. (2022). Surface water, sediment, and biota: The first multi-compartment analysis of microplastics in the Karnafully River, Bangladesh. *Marine Pollution Bulletin*, *180*, 113820. https://doi.org/10.1016/j.marpolbul.2022.113820.

[29] Haque, M.R.; Ali, M.M.; Ahmed, W.; Siddique, M.A.B.; Akbor, M.A.; Islam, M.S.; Rahman, M.M. (2023). Assessment of microplastics pollution in aquatic species (fish, crab, and snail), water, and sediment from the Buriganga River, Bangladesh: An ecological risk. *Science of The Total Environment*, *857*, 159344. https://doi.org/10.1016/j.scitotenv.2022.159344.

[30] Zhao, S.; Kvale, K.F.; Zhu, L.; Zettler, E.R.; Egger, M.; Mincer, T.J.; Stubbins, A. (2025). The distribution of subsurface microplastics in the ocean. *Nature*, *641*(8061), 51–61. https://doi.org/10.1038/s41586-025-08818-1.

[31] Hartz, L.; Grabinski, L.; Salameh, S. (2025). Microplastic pollution in aquatic environments: A meta-analysis of influencing factors and methodological recommendations. *Frontiers in Environmental Science*, *13*, 1600570. https://doi.org/10.3389/fenvs.2025.1600570.

[32] Brennecke, D.; Duarte, B.; Paiva, F.; Caçador, I.; Canning-Clode, J. (2016). Microplastics as vector for heavy metal contamination from the marine environment. *Estuarine, Coastal and Shelf Science*, *178*, 189–195. https://doi.org/10.1016/j.ecss.2015.12.003.

[33] Meng, Q.; Wang, Z.; Shi, F.; Sun, K.; Wen, Z. (2024). Effect of background ions and physicochemical factors on the cotransport of microplastics with Cu^{2+} in saturated porous media. *Scientific Reports*, *14*(1), 27101. https://doi.org/10.1038/s41598-024-78480-6.

[34] De Falco, F.; Gullo, M.P.; Gentile, G.; Di Pace, E.; Cocca, M.; Gelabert, L.; Avella, M. (2018). Evaluation of microplastic release caused by textile washing processes of synthetic fabrics. *Environmental Pollution*, *236*, 916–925. https://doi.org/10.1016/j.envpol.2017.10.057.

[35] Dabrowska, A.; Mielanczuk, M.; Syczewski, M. (2022). The Raman spectroscopy and SEM/EDS investigation of the primary sources of microplastics from cosmetics available in Poland. *Chemosphere*, *308*, 136407. https://doi.org/10.1016/j.chemosphere.2022.136407.

[36] Käppler, A.; Fischer, D.; Oberbeckmann, S.; Schernewski, G.; Labrenz, M.; Eichhorn, K.J.; Voit, B. (2016). Analysis of environmental microplastics by vibrational microspectroscopy: FTIR, Raman or both? *Analytical and Bioanalytical Chemistry*, *408*(29), 8377–8391. https://doi.org/10.1007/s00216-016-9956-3.

[37] Renner, G.; Nellessen, A.; Schwiers, A.; Wenzel, M.; Schmidt, T.C.; Schram, J. (2019). Data preprocessing and evaluation used in the microplastics identification process: A critical review and practical guide. *TrAC Trends in Analytical Chemistry*, *111*, 229–238. https://doi.org/10.1016/j.trac.2018.12.004.

[38] Tajwar, M.; Hasan, M.; Shreya, S.S.; Rahman, M.; Sakib, N.; Gazi, M.Y. (2023). Risk assessment of microplastic pollution in an industrial region of Bangladesh. *Heliyon*, *9*(7), e17949. https://doi.org/10.1016/j.heliyon.2023.e17949.

[39] Manik, M.; Hossain, M.T.; Pastorino, P. (2025). Characterization and risk assessment of microplastics pollution in Mohamaya Lake, Bangladesh. *Journal of Contaminant Hydrology*, *269*, 104487. https://doi.org/10.1016/j.jconhyd.2024.104487.

[40] Shao, H.; Wang, Q.; Wang, L.; Lei, X.; Dai, S.; Li, T.; Mao, X.Z. (2024). Source identification of microplastics in highly urbanized river environments and its implications for watershed management. *Science of the Total Environment*, *950*, 175308. https://doi.org/10.1016/j.scitotenv.2024.175308.